Annals of Physics 420 (2020) 168268

Contents lists available at ScienceDirect

Annals of Physics

journal homepage: www.elsevier.com/locate/aop

Hawking temperature in dispersive media: Analytics and numerics

Alhan Moreno-Ruiz, David Bermudez *

Departamento de Física, Cinvestav, A.P. 14-740, 07000 Ciudad de México, Mexico

ARTICLE INFO

Article history:
Received 25 September 2019
Accepted 12 July 2020
Available online 16 July 2020

Keywords:
Quantum aspects of black holes
Laboratory studies of gravity
Bose–Einstein condensates
Optical fibers
Kerr effect

ABSTRACT

One proposal of analog gravity is that the Hawking effect can be generalized to domains outside of astrophysics. So far, the sonic and the optical systems have been the most successful for this analogy. However, problems arise in analog systems when their dispersive effects are too large to be ignored, as this modifies the usual thermal spectrum of Hawking radiation. A linear approximation of the velocity profile is usually considered to include dispersive effects. In this work, we present new analytical formulas for the Hawking temperature in dispersive media for different velocity profiles beyond the linear approximation and for both the sonic and optical analogs. We check our results with numerical solutions of the wave equation and of the analytical formulas.

1. Introduction

K. Schwarzschild found the first exact solution to the inhomogeneous Einstein equations in general relativity in 1916 [1], this solution hinted on a mysterious object from which nothing can escape, not even light. These objects were eventually called black holes. However, S. Hawking realized in 1974 that if we consider a quantum field on top of the classical background found by Schwarzschild, the black hole produces thermal radiation that escapes to infinity [2,3]. This is the Hawking radiation.

This prediction from forty-six years ago tests our present candidates for quantum theories of gravity. Nevertheless, Hawking radiation rests on some dubious assumptions [4] and has itself not

* Corresponding author.
E-mail addresses: amoreno@fis.cinvestav.mx (A. Moreno-Ruiz), dbermudez@fis.cinvestav.mx (D. Bermudez).
URL: https://www.fis.cinvestav.mx/~dbermudez (D. Bermudez).

https://doi.org/10.1016/j.aop.2020.168268
0003-4916/

passed the ultimate test: experimental verification. In 1981, W. Unruh proposed a way out of this conundrum: to use analog systems to study the Hawking effect [5]. Eventually, this proposal gave birth to a new area of research known as analog gravity.

In analog gravity, phenomena usually related to gravity are studied in different physical systems. The clearest example of this is Hawking radiation itself. Around the event horizon of an astrophysical black hole, the Hawking process leads to the creation of thermal radiation of quantum origin. In analog systems, a process with similar kinetics produces thermal radiation that can be of classical (stimulated) [6] or quantum (spontaneous) [7] origin. The most common analog systems are water tanks [8], Bose–Einstein condensates [9,10], optical fibers [11,12], microcavity polaritons [13], superconducting circuits [14], and fluids of light [15].

The study of analog gravity has given insights into the unclear details of Hawking's derivation [16], such as the role of high-frequency modes, known as the trans-Planckian problem [17]. Its development has also allowed new points of view in the theories of the analog systems. For example, horizon physics predicted new nonlinear effects in optical fibers that have been measured in the search of analog Hawking radiation: negative-frequency resonant radiation [18] and stimulated Hawking radiation of positive [11] and negative [6] frequencies.

Due to dispersion, the derivation of Hawking radiation in analog systems does not suffer from the high-frequency divergences that may occur in the astrophysical case: A frequency shift of any signal causes a change in its group velocity that ultimately leads to a finite frequency shift, unlike the astrophysical case where frequency shifts are infinite. This usually leads to modifications on the Hawking spectrum that are considered under a linear approximation of the velocity profile—equivalent to the curvature of spacetime in astrophysics.

Based on previous work by S. Corley [19], U. Leonhardt and S. Robertson developed an analytical theory that leads to an integral equation to obtain the effective spectrum of Hawking radiation in dispersive media without the previous linear approximation [20]. This equation is hard to solve so only few solutions have been obtained so far. This method considers only the topological nature of the solution of the dispersion relation in the complex plane and it should be related to new approaches by F. Biancalana's group [21,22].

In this paper our goal is three-fold: (1) to expand the analytical theory from the sonic to the optical case and to point out the differences in their derivation; (2) to apply this theory to new velocity profiles, to solve the resulting integrals using Cauchy's residue theorem, and to obtain their analytical Hawking spectrum in terms of an effective temperature (without the linear approximation); and (3) to test our analytical formulas with numerical solutions from the wave equation and from the integrals. Furthermore, we apply a second-order approximation to the commonly used velocity profiles tanh and sech^2 and obtain the spectrum analytically – as an infinite series – and numerically.

2. The analogs of the event horizon

2.1. Schwarzschild spacetime

We consider the movement of light rays around the Schwarzschild radius $r_S = 2GM/c^2$ of a black hole described by the 1+1 Schwarzschild metric in Painlevé-Gullstrand-Lemaître coordinates [23]:

$$\mathrm{d}s^2 = c^2\mathrm{d}t^2 - \left(\mathrm{d}r + \sqrt{\frac{r_S}{r}}c\mathrm{d}t\right)^2. \tag{1}$$

Fig. 1 shows the light-ray trajectories ($\mathrm{d}s^2 = 0$) for outgoing (solid red curves) and ingoing (dashed blue lines) modes. Ingoing modes do not have any peculiar kinematics at r_S, but outgoing modes do: Modes at $r < r_S$ cannot escape from the black hole geometry. These outgoing modes are the main interest in the derivation of Hawking radiation.

We can obtain the same kinematics in Eq. (1) by considering the black-hole spacetime as a moving medium, i.e., as a fluid whose movement is caused by gravity. In the sonic analog, we analyze sound waves in a moving fluid (e.g., Bose–Einstein condensates); in the optical analog,

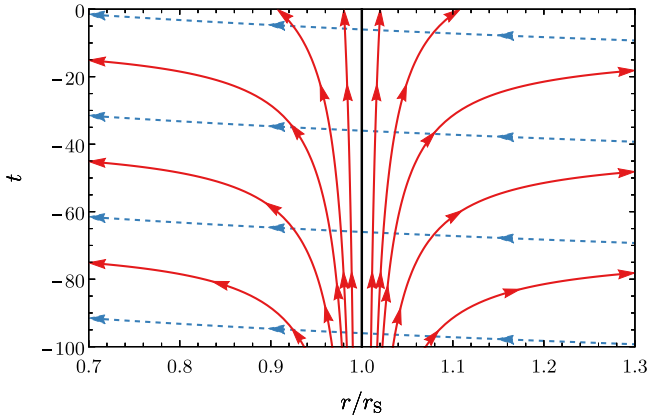

Fig. 1. Geodesics of light rays around the event horizon $r = r_S$ of a Schwarzschild spacetime. Counterpropagating u-modes are shown in solid red and copropagating v-modes in dashed blue. (For interpretation of the references to color in this figure legend, the reader is referred to the web version of this article.)

light waves propagating inside a dielectric material (e.g., in optical fibers). Next, we summarize and compare both analogies.

The Schwarzschild spacetime can be considered as a fluid moving towards the singularity with a varying velocity profile in the radial coordinate given by $c\sqrt{r_S/r}$, such that the fluid velocity at the horizon ($r = r_S$) surpasses the speed of light and traps all light rays inside. We can extend this metric by considering a general velocity profile $u(z)$, as long as it exceeds the limiting speed of the system c (not necessarily the speed of light) at a given point that becomes the analog of the event horizon. The effective metric is then

$$ds^2 = c^2 dt^2 - (dz + u(z)dt)^2 . \tag{2}$$

In the following, we assume that the moving medium moves to the left such that $u < 0$.

2.2. Sonic analog

Let us consider a scalar massless acoustic field in 1+1 dimensions on top a moving fluid with metric (2), i.e., the velocity of the medium varies with position $u = u(z)$. Under certain conditions [24] its Lagrangian can be written as

$$L = \frac{1}{2}\sqrt{-g}g^{\mu\nu}\partial_\mu\phi^*\partial_\nu\phi, \tag{3}$$

where $g^{\mu\nu}$ is the inverse metric tensor and g the determinant of the metric tensor $g_{\mu\nu}$. Using the metric (2), we obtain the wave equation

$$(\partial_t + \partial_z u)(\partial_t + u\partial_z)\phi - c^2\partial_z^2\phi = 0. \tag{4}$$

We define the scalar product for solutions ϕ_1 and ϕ_2 of Eq. (4) as

$$(\phi_1, \phi_2) = \int_{-\infty}^{\infty}\left[\phi_1^*\left(\omega - u\hat{k}\right)\phi_2 - \phi_2\left(\omega - u\hat{k}\right)\phi_1^*\right]. \tag{5}$$

We can generalize the wave equation (4) by including the Bogoliubov dispersion term [25], in that case, the phase velocity is a function of the wavevector $c = c(k)$. As the medium moves to the left ($u < 0$), the counterpropagating waves move to the right and experience a horizon (solid red lines in Fig. 1). The dispersion relation of this medium is

$$\omega - u(z)k = c(k)k, \tag{6}$$

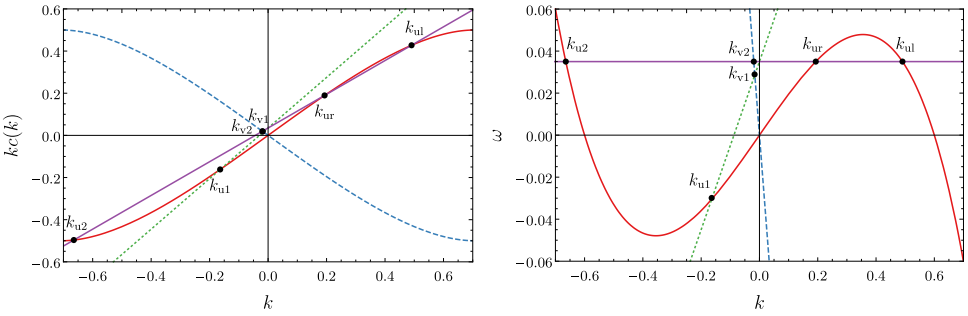

Fig. 2. Dispersion relations for the sonic case in the laboratory frame (left) and the comoving frame (right). The counterpropagating u-modes (solid red) and copropagating v-modes (dashed blue) are matched to two straight lines with the asymptotic velocities, one subsonic u_2 (solid purple) and one supersonic u_1 (dotted green). (For interpretation of the references to color in this figure legend, the reader is referred to the web version of this article.)

and the Bogoliubov dispersion is

$$c(k) = c_0\sqrt{1 - \frac{k^2}{k_0^2}}, \tag{7}$$

where the minus sign corresponds to a subsonic dispersion [26] because the phase velocity $c(k)$ is lower than c_0. As long as the fluid velocity surpasses the speed of sound of the system c_0, a horizon exists for certain frequencies.

In this work, we consider several velocity profiles $u(z)$. For example, the velocity profile of the Schwarzschild metric in Eq. (1) can be taken as

$$u(z) = c\sqrt{\frac{r_S}{z}}. \tag{8}$$

Another example closer to the experimental implementation of sonic analogs [20] is a tanh profile

$$u(z) = \frac{u_2 + u_1}{2} + \left(\frac{u_2 - u_1}{2}\right)\tanh\left(\frac{z}{a}\right), \tag{9}$$

where $u_2 = -0.8$ and $u_1 = -1.2$ are the subsonic and supersonic asymptotic velocities and $a = 1/k_0$ defines the length scale of the velocity change.

We can obtain the asymptotic mode solutions for the dispersion relation as shown in Fig. 2. The counterpropagating u-modes experience the horizon; we show the copropagating v-modes for completeness. The group velocity is $v_g = \partial_k\omega(k) = \partial_k[kc(k)]$, that is, the slope of the solid red and dashed blue curves in Fig. 2 (left). Modes with $v_g > |u|$ propagate to the right (such as k_{ur}) and modes with $v_g < |u|$ propagate to the left (such as k_{ul}). Further solutions k_{u1}, k_{u2} propagate to the left and have negative wavenumbers [27]. It is simpler to study the kinematics from a comoving frame with a given velocity u_2, the dispersion relation in this comoving frame is shown in Fig. 2 (right).

If we consider wavepackets with central position z, wavenumber k, and frequency ω, their dynamics is given by the Hamilton equations [25]:

$$\frac{dz}{dt} = \partial_k\omega = v_g + u, \quad \frac{dk}{dt} = -\partial_z\omega = -k\partial_z u. \tag{10}$$

The group-velocity horizon is defined by the condition $|u| = v_g$.

The phase is given by

$$\varphi = \int (k dz - \omega dt), \tag{11}$$

this is the essential quantity to achieve the phase-matching conditions. We can study how the phase is expressed in different systems to guide us to the conserved quantities. Now, we use this guide to study the optical analog.

2.3. Optical analog

To obtain an optical analog we need a fluid moving close to the speed of light in media, which seems incredibly hard to achieve [28]. However, Leonhardt and colleagues proposed a radical change of mindset [11]: instead of a fast-moving fluid, we send a refractive index perturbation using light pulses and study it in its comoving frame. The change of frame gives kinematic equations of the same form as those from the astrophysical case.

We model the dispersion properties of light inside a fiber with the wavenumber (usually denoted β for fibers) given by

$$\beta(\omega) = \frac{\omega}{c} n(\omega). \tag{12}$$

The simplest dispersion model that contains all horizon physics [12] is

$$\beta(\omega) = \frac{\omega}{c}\sqrt{1 + \frac{\omega^2}{\omega_0^2}}, \tag{13}$$

where the plus sign refers to a subluminal dispersion. Notice that the subluminal dispersion has the opposite sign as the subsonic one considered in Eq. (7). This is not a contradiction, as Eq. (13) defines the wavenumber $\beta(\omega)$ and the phase velocity is its inverse: if β increases as ω increase, then the phase velocity decreases [12,26].

The comoving frame is defined by its velocity. We always choose it as the group velocity of the Kerr perturbation v_{g0}. Then, the propagation time ζ plays the role of time and the delay τ plays the role of distance

$$\tau = t - \frac{z}{v_{g0}}, \qquad \zeta = \frac{z}{v_{g0}}. \tag{14}$$

Under the new coordinates the phase from the sonic case (11) is transformed to the optical one as

$$\varphi = -\int (\omega \mathrm{d}\tau + \omega' \mathrm{d}\zeta), \tag{15}$$

where we have defined the comoving frequency ω' as

$$\omega' = \omega\left(1 - \frac{n(\omega)}{n_{g0}}\right), \tag{16}$$

with $n_{g0} = c/v_{g0}$. As can be seen by comparing Eqs. (11) and (15), the role of k is taken by $-\omega$ and the role of ω by ω'. The dispersion relation in the comoving frame in the optical case (Fig. 3) looks similar to that of the sonic case (Fig. 2 (right)).

A strong light pulse changes the original refractive index of the material n_0 due to the optical Kerr effect [29] as $n = n_0 + \delta n$. We consider that this strong light pulse moves at a constant velocity v_{g0}, for example using fundamental solitons or other pulses whose dynamics is slower than the horizon physics [30]. Then, in the comoving frame waves traveling with $v < v_{g0}$ move in one direction and those with $v > v_{g0}$ in the opposite direction—right and left, respectively—if we use the delay time τ in Eq. (14).

To complete the comparison with the sonic case, we define the dimensionless quantity $v(\tau)$ that acts as the velocity profile for the sonic case

$$v(\tau) = n_{g0} - \delta n(\tau), \tag{17}$$

and depends on the change due to the Kerr effect $\delta n(\tau)$. A comparison of the role that variables play in the sonic and optical systems is shown in Table 1.

Table 1
Relationship between the sonic and optical systems for analog Hawking radiation.

Sonic	Optical
t	ζ
z	τ
k	$-\omega$
ω	ω'
$c(k)$	$n(\omega)$
$u(z)$	$v(\tau)$

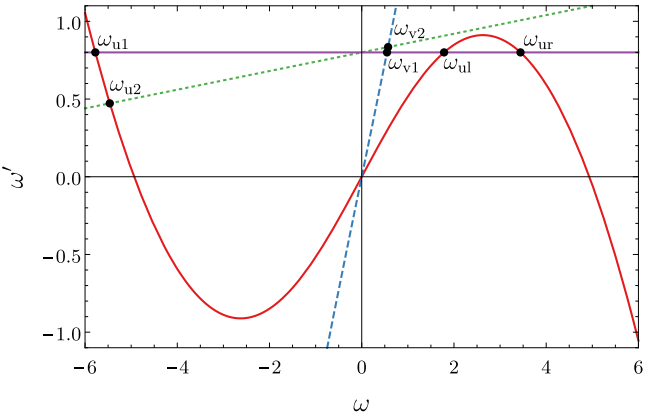

Fig. 3. Dispersion relation for the optical case in the comoving frame. Similar notation as in Fig. 2 for the sonic case. (For interpretation of the references to color in this figure legend, the reader is referred to the web version of this article.)

The Hamilton equations in the comoving frame are

$$\frac{\mathrm{d}\tau}{\mathrm{d}\zeta} = \frac{\omega'}{\omega} - \frac{\omega}{n_{g0}}\partial_\omega n(\omega), \quad \frac{\mathrm{d}\omega'}{\mathrm{d}\zeta} = -\frac{1}{n_{g0}}\partial_\tau \delta n(\tau). \tag{18}$$

In this case, the perturbation $\delta n(\tau)$ defines the velocity profile $v(\tau)$ and it is given by the pulse shape in τ. For example, the most commonly used perturbation in optical analogs is a soliton

$$\delta n(\tau) = \delta n_{\max} \operatorname{sech}^2\left(\frac{\tau}{a}\right). \tag{19}$$

We consider the shape of this perturbation should be localized and fixed in τ, be it solitonic, Gaussian, super-Gaussian, or any other [12].

3. Analytical theory

The quantum vacuum state $|0\rangle$ is defined by the annihilation operator $\hat{a}$ through $\hat{a}|0\rangle = 0, \forall\, \hat{a}$. However, in quantum field theory in curved spaces, the definition of the annihilation operator and the vacuum state can vary in space. This opens the possibility for the creation of particles from vacuum through several mechanisms as the Hawking effect [2], the Unruh effect [31], the dynamical Casimir effect [32], and the Schwinger effect [33]. Some of these processes can be seen as scattering, where it is possible to create particles of positive and negative norms and still fulfill norm conservation.

The existence of negative-norm modes k_{u1}, k_{u2} $[\omega_{u1}, \omega_{u2}]$ defined by the scalar product (5) allows the creation of particles through an analog of the Hawking effect [34]. In terms of the Bogoliubov transformation, the Hawking outgoing-mode is a linear superposition of two ingoing modes with

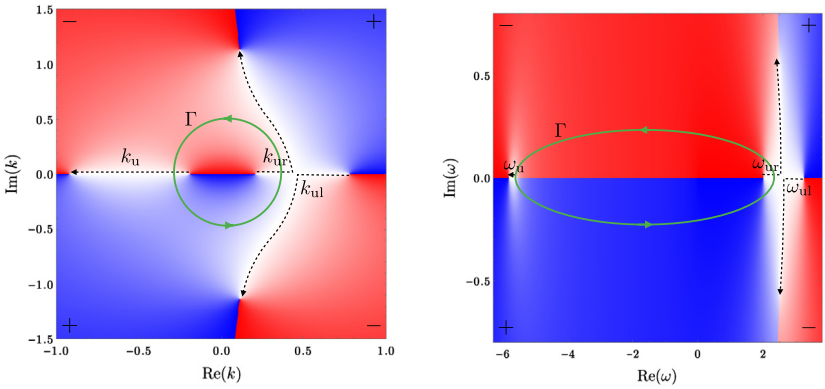

Fig. 4. Complex plane of k for the sonic case (left) and of ω for the optical case (right). The value of Im(z) and Im(τ) is color coded: negative in red, zero in white, and positive in blue. We show the real solutions (black dashed lines) and the integration contour of Eqs. (23) and (24), (green solid ellipses). (For interpretation of the references to color in this figure legend, the reader is referred to the web version of this article.)

opposite norms

$$\phi_{\rm ur}^{\rm out} = \alpha\phi_{\rm ul}^{\rm in} + \beta\phi_{\rm u1}^{\rm in}. \tag{20}$$

From the scalar product (5), the norm for the normalized mode $\phi_{\rm ur}^{\rm out}$ is

$$1 = |\alpha|^2 - |\beta|^2, \tag{21}$$

and if $|\beta| > 0$ there is a norm amplification that can lead to particle creation. If the vacuum state is amplified by a horizon, the resulting radiation is the analog of the Hawking radiation [3]. In the dispersionless case, this radiation is in a thermal state described by

$$\left|\frac{\beta}{\alpha}\right|^2 = \exp\left(-\frac{\hbar\omega}{k_B T}\right), \tag{22}$$

where $\hbar$ is the reduced Planck constant and k_B is the Boltzmann constant. For dispersive cases, the horizon becomes fuzzy in position z [τ], which can be seen in numerical solutions of Hamilton equations in Eq. (10) [Eq. (18)]. In this case it is better to characterize the horizon in the conjugated space k [ω].

Leonhardt and Robertson [20] showed that the Hawking effect connects positive and negative norm modes in the complex plane. They developed an equation to calculate the Hawking temperature in sonic systems with dispersion. The relative phase k of the Bogoliubov coefficients in the complex plane given by Eq. (22) is connected to a contour integral in position z, see Fig. 4 (left). This equation is

$$k_B T = \frac{i\hbar\omega}{\oint_\Gamma z(k)\mathrm{d}k}. \tag{23}$$

The proof of this equation is performed in the complex conjugated space using the saddle-point approximation and can be found in Appendix A of Ref. [20].

We obtain an equivalent equation for the optical case by following the transformations in Section 2.3. In this case, the complex plane is in the laboratory frequency ω and the integration is in delay time τ,

$$k_B T = \frac{i\hbar\omega}{\oint_\Gamma \tau(\omega)\mathrm{d}\omega}. \tag{24}$$

Table 2
Hawking temperature for growing profiles in the sonic case (left) and the optical case (right). We define $v_{pr}(\omega) = v_{g0} - c(\omega)$ and $v_{gr}(\omega) = v_{g0} - v_g(\omega)$.

$u(z)$	T/T_0	$\delta n(\tau)$	T/T_0
z	1	τ	1
$z^{1/2}$	$\frac{c(k)}{v_g(0)}$	$\tau^{1/2}$	$\frac{v_{pr}(\omega)}{v_{gr}(0)}$
$z^{1/3}$	$\frac{c^2(k)}{v_g^2(0)}\left(1+\frac{kc(k)v_g'(0)}{2v_g^2(0)}\right)^{-1}$	$\tau^{1/3}$	$\frac{v_{pr}^2(\omega)}{v_{gr}^2(0)}\left(-1+\frac{\omega v_{pr}(\omega)v_{gr}'(0)}{2v_{gr}^2(0)}\right)^{-1}$

Fig. 4 shows differences and similarities of the complex plane and the integration of the sonic and optics cases: these integrals have the same form because the topological structure of $\tau(\omega)$ is the same as $z(k)$ as shown in the figure, it is also why we connect the supersonic and subluminal dispersions [21].

In the next section, we obtain the analytical Hawking temperature for general velocity profiles $z^{\pm 1/n}$ (sonic) and $\tau^{\pm 1/n}$ (optical). Two formulas for sonic analogs derived in Ref. [20] are included as particular cases, including the Schwarzschild spacetime, but the rest are new analytical results from this work.

We also develop an equation for a second-order approximation that can be used to obtain more detailed spectra in physical applications. In particular, we present results for a tanh and a sech^2 profiles for the sonic case. These results are limited because – as we will see next – the analytical formula is given as an infinite series and is valid only when a convergence condition is fulfilled.

4. Analytical Hawking temperature

We can solve integrals (23) and (24) analytically for profiles of the form $z^{\pm 1/n}$ or $\tau^{\pm 1/n}$ by using Cauchy's integral theorem. It is convenient to divide these integrals in growing and decaying profiles, i.e., if they grow or decay to the right side of the profile, as the method of solution depends on this behavior (determined by the sign of the exponent: $+$ for growing and $-$ for decaying). In this section we present the derivation for general growing $z^{1/n}$ and decaying $z^{-1/n}$ profiles, but we work out explicitly six specific cases in Appendix. We only show the sonic case, as the analytic integrals are solved in the same way for the optical case, due to the topological nature of the integral equation.

4.1. Growing profiles

We can solve the integral for the sonic case given by Eq. (23) for the velocity profiles expressed in the general form

$$u(z) = u_0 \left(\frac{z}{a}\right)^{1/n}, \tag{25}$$

where u_0, a are constants that define the scale of the profile and $n \in \mathbb{Z}$. For example, the results for z, $z^{1/2}$ and $z^{1/3}$ are shown in Table 2 (left). We also calculated the analytical formulas for $z^{1/4}$ and $z^{1/5}$, but we do not present the formulas here, as they are too long.

Similarly, for optical profiles in the general form

$$\delta n(\tau) = \delta n_0 \left(\frac{\tau}{a}\right)^{1/n}, \tag{26}$$

the cases τ, $\tau^{1/2}$, and $\tau^{1/3}$ are shown in Table 2 (right). For simplicity, the results are expressed in terms of the velocities relatives to the perturbation: the relative phase-velocity $v_{pr}(\omega) = v_{g0} - c(\omega)$ and the relative group-velocity $v_{gr}(\omega) = v_{g0} - v_g(\omega)$.

The resulting spectra are shown in terms of their effective Hawking temperature in Fig. 5. A thermal emission has a constant temperature throughout its spectra—as the $\propto z$ and $\propto \tau$ cases. The

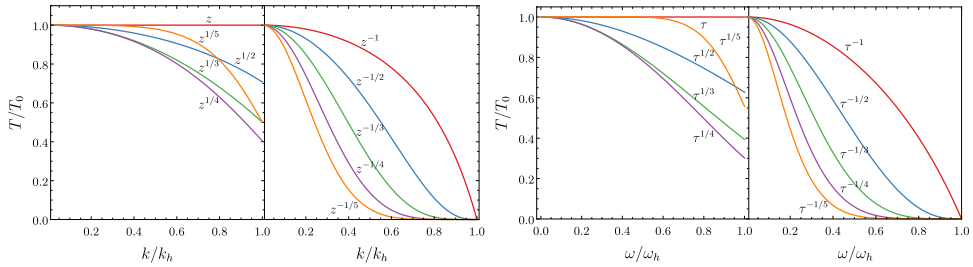

Fig. 5. Hawking temperature for the sonic (left) and optical (right) cases. For both cases we show growing $z^{1/n}$, $\tau^{1/n}$ and decaying $z^{-1/n}$, $\tau^{-1/n}$ profiles.

plots for the sonic [optical] analog are on the left [right], where the growing and decaying profiles are shown. The axes are normalized to the horizon wavenumber [frequency] and the thermal Hawking temperature. As the velocity profiles deviate from the linear case, their spectra also depart from thermality, as shown in Fig. 5 (left). This is because the Hawking temperature depends on $c(k)$ or $v_{pr}(\tau)$ and the different velocity profiles.

An attentive reader may be wondering why the Schwarzschild case $\propto z^{-1/2}$ is not thermal. The thermality of this profile is only for a dispersionless background, as it is the case for astrophysical spacetime in General Relativity. This was first shown by T. Jacobson [35]. If the astrophysical spacetime has dispersion – e.g., at the Planck scale – then the Hawking spectrum is not thermal even for the Schwarzschild case, although it would still be a good approximation for wavelengths longer than the Planck length, i.e., for basically any conceivable measurement. However, the spectrum for the $z^{1/5}$ [$\tau^{1/5}$] profile are closer to thermality ($T = T_0$) than expected.

Now we show the derivation of the analytic Hawking temperature for a growing velocity profile of the form

$$u(z) = u_0 \left(\frac{z}{a}\right)^{1/n}. \tag{27}$$

From the dispersion relation in Eq. (6) we have $u(z) = \omega/k - c(k)$ and by eliminating $u(z)$ we obtain

$$z(k) = \frac{a u_0^n k^n}{(\omega - c(k)k)^n}. \tag{28}$$

We develop the denominator in series around the wavenumber k_0 that fulfills $k_0 c(k_0) - \omega = 0$, i.e., the dispersion relation at $z = 0$. We only consider the first n terms of the series as they are the only ones contributing to the integral

$$z(k) = \frac{a u_0^n k^n}{\sum_{j=1}^{n} \frac{v_g^{j-1}(k_0)}{j!}(k - k_0)^j}. \tag{29}$$

Using the residuals of the integral we have

$$\frac{\hbar\omega}{k_B T} = \frac{2\pi a u_0^n}{v_g^n(k_0)(n-1)!}\, \partial_k^{n-1} \left(\frac{k^n}{\sum_{j=1}^{n} \frac{v_g^{(j-1)}(k_0)}{j! v_g(k_0)}(k - k_0)^{j-1}} \right)\Bigg|_{k=k_0}. \tag{30}$$

At the phase horizon $c(k_0) = |u(z_0)|$ we can define the surface gravity as

$$\alpha = \partial_z u(z)|_{z_\infty} = \frac{c^{n+1}(k_0)}{n a u_0^n}, \tag{31}$$

Table 3
Hawking temperature for decaying profiles for the sonic case (left) and for the optical case (right).

$u(z)$	T/T_0	$\delta n(\tau)$	T/T_0
z^{-1}	$\frac{v_g(k)}{c(k)}$	τ^{-1}	$\frac{v_{gr}(\omega)}{v_{pr}(\omega)}$
$z^{-1/2}$	$\frac{v_g^2(k)}{c^2(k)}\left(1-\frac{kv_g'(k)}{2v_g(k)}\right)^{-1}$	$\tau^{-1/2}$	$\frac{v_{gr}^2(\omega)}{v_{pr}^2(\omega)}\left(1-\frac{\omega v_{gr}'(\omega)}{2v_{gr}(\omega)}\right)^{-1}$
$z^{-1/3}$	$\frac{v_g^3(k)}{c^3(k)}\left(1-\frac{3kv_g'^2(k)}{2v_g^2(k)}+\frac{k^2}{6v_g^2(k)}[3v_g'^2(k)-v_g(k)v_g''(k)]\right)^{-1}$	$\tau^{-1/3}$	$\frac{v_{gr}^3(\omega)}{v_{pr}^3(\omega)}\left(1-\frac{3\omega v_{gr}'(\omega)}{2v_{gr}(\omega)}+\frac{\omega^2}{6v_{gr}^2(\omega)}[3v_{gr}'^2(\omega)-v_{gr}(\omega)v_{gr}''(\omega)]\right)^{-1}$

and use it to simplify Eq. (30). The Hawking temperature is then

$$T=T_0\frac{v_g^n(k_0)}{c^n(k_0)}k_0 n!\left[\partial_k^{n-1}\left(\frac{k^n}{\sum_{j=1}^n\frac{v_g^{(j-1)}(k_0)}{j!v_g(k_0)}(k-k_0)^{j-1}}\right)\bigg|_{k=k_0}\right]^{-1}, \tag{32}$$

where T_0 is the usual Hawking temperature

$$T_0=\frac{\hbar\alpha}{2\pi k_B}. \tag{33}$$

Eq. (32) can be solved for different cases. For $n=1,2,3$, the solutions are given explicitly in Table 2 and worked out in the Appendix in Eqs. (A.4), (A.10), and (A.15).

4.2. Decaying profiles

We can also solve the integrals in Eqs. (23) and (24) for the velocity profiles in the general form

$$u(z)=u_0\left(\frac{a}{z}\right)^{1/n},\quad u(\tau)=u_0\left(\frac{a}{\tau}\right)^{1/n}, \tag{34}$$

where again the constants define the scale of the profiles. For example, solving the integral of Eq. (23), the Hawking temperature for the first three profiles z^{-1}, $z^{-1/2}$ and $z^{-1/3}$ are shown in Table 3 (left). Similarly, the integral of Eq. (24) for optical profiles is solved for profiles τ^{-1}, $\tau^{-1/2}$ and $\tau^{-1/3}$ and are shown in Table 3 (right). We can solve further profiles $z^{-1/4}$ and $z^{-1/5}$, but we do not present the analytic results here due to their length.

The plots in Fig. 5 show the results for the decaying profiles, where no thermal spectrum is found. Still, as the velocity profile gets further away from 1, i.e., the spectrum becomes less thermal, and in fact for decaying profiles it is always zero at the horizon. This is explained by the factor v_g^n/c^n for the sonic case [v_{gr}^n/v_{pr}^n for the optical case] that appears in the effective temperature for the $z^{1/n}$ [$\tau^{1/n}$] profile in Table 3. This factor goes to zero at the horizon k_h [ω_h], as the group velocity is zero at the horizon and the phase velocity is not. For the decaying cases, the dispersion is more important with higher roots as it departs faster from thermality, continuing the trend seen in the analytical cases. In this case, the case $z^{-1/5}$ [$\tau^{-1/5}$] behaves as expected.

To obtain the analytical solution for a decaying profile of the form

$$u(z)=-u_0\left(\frac{a}{z}\right)^{1/n}, \tag{35}$$

with $n\in\mathbb{Z}$, we solve the dispersion relation as

$$z=\frac{au_0^n k^n}{(kc(k)-\omega)^n}. \tag{36}$$

We expand the denominator around the wavenumber k_∞, the solution of the dispersion relation for $z \to \infty$, keeping only the first n terms, as they are the nonzero ones in the integral

$$kc(k) - \omega = \sum_{j=1}^{n} \frac{1}{j!} v_g^{(j-1)}(k_\infty)(k - k_\infty)^j. \tag{37}$$

This solution has n poles, however, only the simple pole at k_∞ contributes to the integral. We get from Cauchy's residue theorem

$$\frac{\hbar\omega}{k_B T} = \frac{2\pi}{(n-1)!} \frac{u_0^n}{v_g^n(k_\infty)} \partial_k^{n-1} \left[k^n \left(\sum_{j=1}^{n} \frac{1}{j!} \frac{v_g^{(j-1)}(k_\infty)}{v_g(k_\infty)} (k - k_\infty)^{j-1} \right)^{-1} \right]^n \Bigg|_{k=k_\infty}. \tag{38}$$

We calculate the surface gravity from the velocity profile at the phase horizon

$$\alpha = \partial_z u(z)|_{z_\infty} = \frac{c^{n+1}(k_\infty)}{n a u_0^n}. \tag{39}$$

With this, we can simplify the Hawking temperature to

$$T = T_0 \frac{v_g^n(k)}{c^n(k)} n! k \left[\partial_k^{n-1} k^n \left(\sum_{j=1}^{n} \frac{1}{j!} \frac{v_g^{(j-1)}(k_\infty)}{v_g(k_\infty)} (k - k_\infty)^{j-1} \right)^{-1} \right]^n \Bigg|_{k=k_\infty}. \tag{40}$$

4.3. Second-order approximation

Let us consider now a second-order velocity profile in the sonic case

$$u(z) = \alpha_1 z + \alpha_2 z^2. \tag{41}$$

The dispersion relation (6) together with the binomial theorem leads to

$$z(k) = -\frac{\alpha_1}{2\alpha_2} \pm 2 \sum_{m=0}^{\infty} a(m) \left(\frac{\omega}{k} - c(k) \right)^m, \tag{42}$$

where

$$a(m) = \frac{(-1)^{m-1}}{2^m} \frac{(2m-3)!!}{m!(m-1)!} \frac{(4\alpha_2)^{m-1}}{\alpha_1^{2m-1}}. \tag{43}$$

In this case, the integral in Eq. (23) can only be solved as an infinite series and the Hawking temperature can be formally expressed as

$$T = \frac{\hbar\omega}{4\pi k_B} \left[\sum_{m=1}^{\infty} a(m) \partial_k^{m-1} \left(\omega - kc(k) \right)^m \Big|_{k=0} \right]^{-1}. \tag{44}$$

The necessary condition for the convergence of the series (44) is

$$\lim_{m\to\infty} \left| \frac{4\alpha_2(2m-1)}{\alpha_1^2(m^2+m)} \frac{\partial_k^m [\omega - kc(k)]^{m+1}}{\partial_k^{m-1} [\omega - kc(k)]^m} \right| < 1. \tag{45}$$

For the optical case the formula is similar, with the usual changes

$$T = \frac{\hbar\omega'}{4\pi k_B} \left[\sum_{m=1}^{\infty} a(m) \partial_\omega^{j-1} \left(\omega' - \frac{\omega v_{pr}(\omega)}{c} \right)^j \Bigg|_{\omega=0} \right]^{-1}. \tag{46}$$

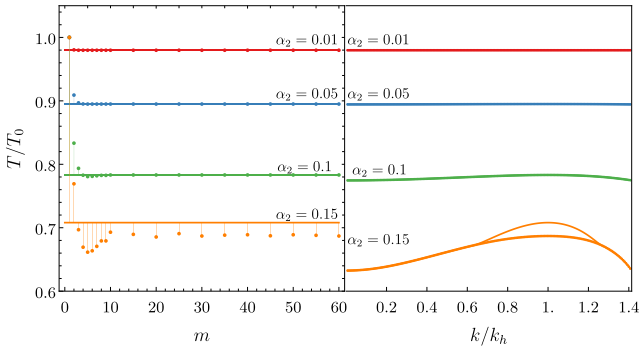

Fig. 6. Hawking temperature for the second-order profile $\alpha_1 z + \alpha_2 z^2$ with $\alpha_1 = 1$, several values of α_2, evaluated at the group-velocity horizon k_h, and with m terms of the series (left). Hawking spectrum for the second-order profile with 60 terms (right). The lines indicate the numerical solution.

This result is only valid when the following condition is fulfilled

$$\lim_{m\to\infty} \left| \frac{4\alpha_2(2m-1)}{\alpha_1^2(m^2+m)} \frac{\partial_\omega^m \left(\omega' - \omega v_{pr}(\omega)/c\right)^{m+1}}{\partial_\omega^{m-1} \left(\omega' - \omega v_{pr}(\omega)/c\right)^{m}} \right| < 1. \tag{47}$$

The series can be calculated analytically via symbolical software, we calculated up to 60 terms of the series. In Fig. 6 (left), a study of the convergence is shown at the group-velocity horizon, the most problematic area. If the value in Eq. (45) is much smaller than 1, the convergence is fast, however, if it is closer to 1 the series (points) converges to a different value than the numerical solution (line). Furthermore, note that the first term of all series is 1 as expected to match the linear approximation. In Fig. 6 (right) we studied the full spectra for several values of α_1, α_2, we see that the series converges to the analytical value except for large α_2 around the group-velocity horizon k_h. Moreover, for the limiting linear case $\alpha_2 \to 0$, the spectrum becomes thermal as expected, but if α_2 increases, the thermality is initially kept (constant T/T_0), although the temperature decreases ($T/T_0 < 1$). For even higher values of α_2, the thermality is finally lost and the wavenumber k_h dominates the spectrum.

4.4. Second-order approximation to physical profiles

In the analytical studies of Hawking radiation a linear approximation is usually taken, i.e., the spectrum is calculated considering that the velocity profile is linear $\propto z$ [25,36,37] or $\propto \tau$ [6,11], and from there, the famous formulas for the Hawking temperature in analog systems are obtained

$$T = \frac{\hbar}{2\pi k_B} \left.\frac{\mathrm{d}u}{\mathrm{d}z}\right|_h, \qquad T = \frac{\hbar}{2\pi k_B} \left.\frac{1}{\delta n}\frac{\mathrm{d}\delta n}{\mathrm{d}\tau}\right|_h. \tag{48}$$

In this work using the analytical formulas in Eqs. (23) and (24) in terms of the integral in the complex plane, we obtained the Hawking temperature considering a second-order approximation given by Eqs. (44) and (46). We apply these formulas in the convergence region for the most used velocity profiles tanh in Eq. (9) and sech^2 in Eq. (19) and obtain the difference with the linear profile. These velocity profiles together with the linear approximation form the base model for analog Hawking radiation.

Finally, we compare our results with numerical solutions and obtain a good match as long as the series converges; these results are shown in Fig. 7. As expected, the spectra are thermal for low wavenumbers.

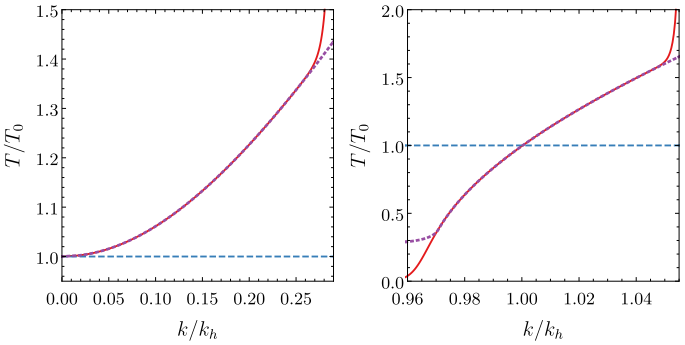

Fig. 7. Hawking temperature for the tanh profile around $z = 0$ (left) and the sech^2 around the zero curvature point (right). We show the analytical result for the first- (dashed blue) and second-order (solid red) approximations and the numerical result (dotted purple).

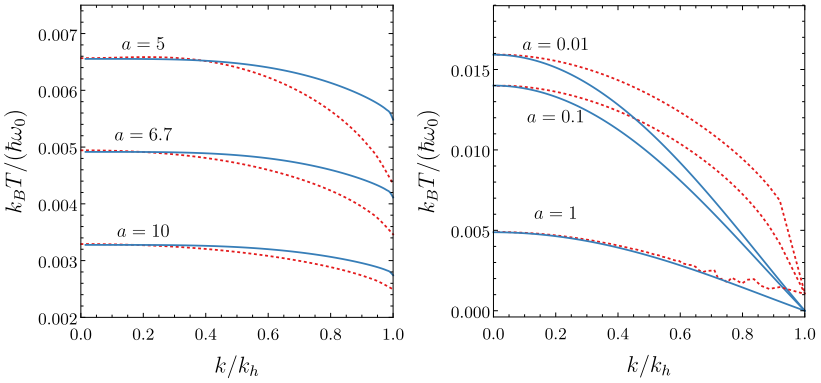

Fig. 8. Hawking temperature for a tanh (left), and inverse z^{-1} (right) profiles obtained from the analytical formula (23) (solid blue line) and from numerically solving the wave equation (dotted red line).

5. Numerical Hawking temperature

Now we perform two different numerical checks on our analytical calculations: first, we calculate the effective Hawking temperature by directly the wave equation (4) to check the validity of the approximations used to derive the integral formulas (23) and (24), and second, we perform numerical integrals to check that our calculations for the different velocity profiles are correct, i.e., checking the implementation of the integral formulas.

For the first case, we numerically solve the wave equation in position space (4) for the Hawking outgoing-mode in Eq. (20). With the solution in the asymptotic region, we can obtain the Bogoliubov coefficients α and β and the Hawking temperature from Eq. (22). The results for the tanh and z^{-1} profiles are shown in Fig. 8. In this way, we validate the approximations used to derive the integral equations: these two completely different approaches match for the dispersionless limit of low wavenumbers, and they differ for higher wavenumbers, in particular the numerical errors are very large close to the horizon wavenumber k_h. Also, the numerical results are better for the tanh profile as it converges faster to its asymptotic values. It was not clear if the method would work for the $z^{\pm 1/n}$-profiles studied here as one asymptotic value is infinite, Fig. 8 (right) shows the result for the z^{-1}-profile.

For the second case, we can check our analytical calculations for the several velocity profiles by performing numerical integrals to calculate the spectra. The numerical integration is performed

in Cartesian coordinates, the trajectory is either an ellipse or a rectangle that contains the origin and never crosses any branch cuts in the complex plane; similar to the green contours shown in Fig. 4. One way to keep track that our analytical method is working correctly is that the real part of the integral in Eqs. (23) and (24) is zero. If this is not the case, one of the main issues in the numerical integrals was finding the appropriate contour. Once chosen correctly, the real part and the difference with the analytical method were of the order of $\sim 10^{-15}$. The numerical results give the same plot as Fig. 5 for all cases and are not shown again.

6. Conclusions

We extended the analytical theory given by Leonhardt and Robertson [20] from the sonic to the optical case. We solved analytically the resulting integral for new velocity profiles and found the conditions for thermality. As expected, all of them are thermal for low wavenumbers [frequencies] in the sonic [optical] case.

The Hawking temperature can also be obtained numerically from the wave equation for a Hawking out-mode. The comparison with the analytical formula validates the approximations used to derive it. The analytical calculations using the integral formula can be validated by solving the integrals numerically; these evaluations match our analytical results. The analytical and numerical studies confirm some unusual behavior for growing profiles that deserve further research.

For the optical case, we found a similar formula for the Hawking temperature given in Eq. (24). The solutions of the optical case in the complex plane are topologically equivalent to those in the sonic one. This leads to similar equations with a convenient choice of parameters and functions to describe the optical system. We solved the integral for growing and decaying perturbations analytically and numerically with excellent agreement.

We also obtained an analytical formula for the second-order velocity profile, although in this case the result is given as an infinite series. We obtained the first 60 terms of the series and studied its convergence properties: the series converges when it fulfills conditions (45) or (47) and its result matches the numerical solution.

These analytical formulas are complicated but they do not use the ubiquitous linear approximation for velocity profiles in dispersive systems. In this way, we can use these formulas to test this approximation and see where it fails. For the sech profile commonly used in optics, the profiles agree qualitatively but not quantitatively.

In analog theories, the quantities that define the dispersion length are the constants k_0 for the sonic and Ω_0 for the optical cases. These constants are related to the microscopic structure of the dispersive material that is perceived as a dispersion for large energies. Something similar could happen in real spacetime. If spacetime is dispersive, its microscopic structure would be given by the Planck length and the dispersive effects could be felt for modes of comparable wavelengths or smaller. This would mean that even for the Schwarzschild spacetime the Hawking radiation would not be thermal for all wavelengths, only to wavelengths longer than the Planck length. For a Schwarzschild profile ($z^{-1/2}$) with the dispersion, the Hawking temperature starts as the expected Hawking temperature T_0, but it is not the same for all wavelengths, it actually goes to zero at the horizon [35].

CRediT authorship contribution statement

Alhan Moreno-Ruiz: Performed the analytic and numerical calculations, Wrote and reviewed the manuscript. **David Bermudez:** Proposed the project, Supervised the calculations, Wrote and reviewed the manuscript.

Declaration of competing interest

The authors declare that they have no known competing financial interests or personal relationships that could have appeared to influence the work reported in this paper.

Acknowledgments

We would like to acknowledge the useful discussions with Scott Robertson and Ulf Leonhardt. We also appreciate the valuable comments and corrections from the anonymous reviewer. We acknowledge funding by SEP-Cinvestav (Mexico), project 2018–60. AMR acknowledges funding by Conacyt (Mexico) scholarship 786398.

Appendix. Analytic spectra calculations

In this Appendix we work out the method to obtain the analytical Hawking spectrum for several velocity profiles. We formulate the sonic case, but the optical one is analogous.

A.1. Profile z

A linear velocity profile is

$$u(z) = u_0 \frac{z}{a} = \alpha z. \tag{A.1}$$

From the dispersion relation in Eq. (6), we have $u(z) = \omega/k - c(k)$ and by eliminating $u(z)$ we obtain

$$z(k) = \frac{\omega}{\alpha k} - \frac{c(k)}{\alpha}. \tag{A.2}$$

Considering that $c(k)$ is an analytic function, the contour integral for the effective temperature (23) is then

$$\int_\Gamma z(k)\mathrm{d}k = \int_\Gamma \left(\frac{\omega}{\alpha k} - \frac{c(k)}{\alpha}\right)\mathrm{d}k = \frac{\omega}{\alpha}\int_\Gamma \frac{\mathrm{d}k}{k}. \tag{A.3}$$

Finally, the Hawking temperature is

$$T = \frac{\hbar\alpha}{2\pi k_B} \equiv T_0, \tag{A.4}$$

this is, the spectrum is thermal even with dispersion.

A.2. Profile $z^{1/2}$

For a square-root velocity profile

$$u(z) = u_0 \left(\frac{z}{a}\right)^{1/2}, \tag{A.5}$$

and the dispersion relation (6) we have

$$z(k) = \frac{a}{(u_0 k)^2}(\omega - kc(k))^2. \tag{A.6}$$

This function has a simple pole in $k = 0$, by Cauchy's integral theorem we can integrate

$$\frac{\hbar\omega}{k_B T} = -\frac{4\pi\omega a v_g(0)}{u_0^2}. \tag{A.7}$$

We also have $u(0) = 0$, then from the dispersion relation we define k_0 as the solution of the dispersion relation that moves to the left k_{ul} and from there $k_0 c(k_0) = \omega$. The magnitude of the phase velocity at the phase horizon z_0, is the same as the fluid velocity

$$c(k_0) = |u(z_0)| = u_0 \left(\frac{z_0}{a}\right)^{1/2}. \tag{A.8}$$

We define the surface gravity α of the system as

$$\alpha = \partial_z u(z)|_{z_0} = -\frac{u_0}{(a z_0)^{1/2}}. \tag{A.9}$$

From the last two equations we obtain a relation between a and α to simplify the effective temperature to

$$T = T_0 \frac{c(k_0)}{v_g(0)}. \tag{A.10}$$

This is the value presented in Table 2, where $k_0 \to k$, as they refer to the unperturbed values of the dispersion relation.

A.3. Profile $z^{1/3}$

For a cubic-root velocity profile

$$u(z) = u_0 \left(\frac{z}{a}\right)^{1/3}, \tag{A.11}$$

the dispersion relation (6) leads to

$$z(k) = \frac{a}{(u_0 k)^3}(\omega - kc(k))^3. \tag{A.12}$$

This function has a simple pole in $k = 0$, by Cauchy's integral theorem we have

$$\frac{\hbar\omega}{k_B T} = -\frac{6\pi\omega a v_g^2(0)}{u_0^3}\left(1 + \frac{\omega v_g'(0)}{2v_g^2(0)}\right). \tag{A.13}$$

Following the same steps as in the previous case with $c(k_0) = |u(z_0)|$, the surface gravity is

$$\alpha = -\frac{u_0}{3(az_0^2)^{1/3}}. \tag{A.14}$$

Then we can simplify the effective temperature to

$$T = T_0 \frac{c^2(k_0)}{v_g^2(0)}\left(1 + \frac{c(k_0)k_0 v_g'(0)}{2v_g^2(0)}\right)^{-1}, \tag{A.15}$$

as presented in Table 2.

A.4. Profile z^{-1}

For an inverse velocity profile

$$u(z) = -u_0 \frac{a}{z}, \tag{A.16}$$

and from the dispersion relation we get

$$z(k) = \frac{a u_0 k}{kc(k) - \omega}. \tag{A.17}$$

The only pole is in $z \to \infty$, where the velocity of the medium is zero $\omega = c(k_\infty)k_\infty$. Then, the integral is

$$\frac{\hbar\omega}{k_B T} = 2\pi \frac{a u_0 k_\infty}{v_g(k_\infty)}, \tag{A.18}$$

and using the dispersion at infinity, we can calculate the surface gravity as

$$\alpha = \partial_z u(z)|_{z_\infty} = \frac{c^2(k_\infty)}{a u_0}, \tag{A.19}$$

and then simplify the spectrum to

$$T = T_0 \frac{v_g(k_\infty)}{c(k_\infty)}. \tag{A.20}$$

A.5. Profile $z^{-1/2}$

For the Schwarzschild profile or inverse square-root velocity profile

$$u(z) = -u_0 \left(\frac{a}{z}\right)^{1/2}, \tag{A.21}$$

and from the dispersion relation we get

$$z(k) = \frac{a u_0^2 k^2}{(\omega - kc(k))^2}. \tag{A.22}$$

This function has two poles, but only one contributes to the integral at $z \to \infty$, which results in

$$\frac{\hbar\omega}{k_B T} = \frac{a u_0^2}{v_g^3(k_\infty)}(2v_g(k_\infty)k_\infty - v_g'(k_\infty)k_\infty^2). \tag{A.23}$$

Again we calculate the surface gravity at the phase horizon

$$\alpha = \partial_z u(z)|_{z_\infty} = \frac{c^3(k_\infty)}{2a u_0^2}, \tag{A.24}$$

to simplify the Hawking spectrum to

$$T = T_0 \frac{v_g^2(k_\infty)}{c^2(k_\infty)} \left(1 - \frac{v_g'(k_\infty)k_\infty}{2v_g(k_\infty)}\right)^{-1}. \tag{A.25}$$

This means that the velocity profile of Schwarzschild spacetime is not thermal in a dispersive medium.

A.6. Profile $z^{-1/3}$

For the inverse cubic-root velocity profile

$$u(z) = -u_0 \left(\frac{a}{z}\right)^{1/3}, \tag{A.26}$$

and from the dispersion relation we get

$$z(k) = \frac{a u_0^3}{(\omega/k - c(k))^3}. \tag{A.27}$$

This function has three poles, but again the one that contributes to the integral is at $z \to \infty$, the result is

$$\frac{\hbar\omega}{k_B T} = 2\pi \frac{3k_\infty a u_0^3}{v_g^3(k_\infty)} \left[1 + \frac{k_\infty^2 v_g^2(k_\infty)}{2v_g(k_\infty)} - \frac{k_\infty}{6v_g^2(k_\infty)}(9v_g'(k_\infty) + k_\infty v_g''(k_\infty))\right]. \tag{A.28}$$

The surface gravity at the phase horizon

$$\alpha = \partial_z u(z)|_{z_\infty} = \frac{c^4(k_\infty)}{3a u_0^3}, \tag{A.29}$$

can be used to simplify the Hawking spectrum to

$$T = T_0 \frac{v_g^3(k)}{c^3(k)} \left(1 - \frac{3v_g'^2(k)k}{2v_g^2(k)} + \frac{k^2}{6v_g^2(k)}[3v_g'(k)^2 - v_g''(k)v_g(k)]\right)^{-1}. \tag{A.30}$$

References

[1] K. Schwarzschild, Sitzungsber. Preuss. Akad. Wiss. Berlin (Math. Phys.) 1916 (1916) 189–196, arXiv:physics/9905030.
[2] S.W. Hawking, Nature 248 (5443) (1974) 30–31, http://dx.doi.org/10.1038/248030a0.
[3] S.W. Hawking, Comm. Math. Phys. 43 (3) (1975) 199–220, http://dx.doi.org/10.1007/BF02345020.
[4] A.D. Helfer, Rep. Progr. Phys. 66 (2003) 943–1008, http://dx.doi.org/10.1088/0034-4885/66/6/202.
[5] W.G. Unruh, Phys. Rev. Lett. 46 (21) (1981) 1351–1353, http://dx.doi.org/10.1103/PhysRevLett.46.1351.
[6] J. Drori, Y. Rosenberg, D. Bermudez, Y. Silberberg, U. Leonhardt, Phys. Rev. Lett. 122 (1) (2019) 010404, http://dx.doi.org/10.1103/PhysRevLett.122.010404.
[7] J.R.M. de Nova, K. Golubkov, V.I. Kolobov, J. Steinhauer, Nature 569 (2019) 688–691, http://dx.doi.org/10.1038/s41586-019-1241-0.
[8] G. Rousseaux, C. Mathis, P. Maïssa, T.G. Philbin, U. Leonhardt, New J. Phys. 10 (5) (2008) 053015, http://dx.doi.org/10.1088/1367-2630/10/5/053015.
[9] C. Barceló, M. Visser, Classical Quantum Gravity 18 (6) (2001) 1137–1156, http://dx.doi.org/10.1088/0264-9381/18/6/312.
[10] J. Steinhauer, Nat. Phys. 12 (2016) 959–965, http://dx.doi.org/10.1038/nphys3863.
[11] T.G. Philbin, C.E. Kuklewicz, S. Robertson, S. Hill, F. König, U. Leonhardt, Science 319 (5868) (2008) 1367–1370, http://dx.doi.org/10.1126/science.1153625.
[12] D. Bermudez, U. Leonhardt, Phys. Rev. A 93 (5) (2016) 053820, http://dx.doi.org/10.1103/PhysRevA.93.053820.
[13] H.S. Nguyen, D. Gerace, I. Carusotto, D. Sanvitto, E. Galopin, A. Lemaître, I. Sagnes, J. Bloch, A. Amo, Phys. Rev. Lett. 114 (2015) 036402, http://dx.doi.org/10.1103/PhysRevLett.114.036402.
[14] P. Nation, J. Johansson, M. Blencowe, F. Nori, Rev. Modern Phys. 84 (1) (2012) 1–24, http://dx.doi.org/10.1103/RevModPhys.84.1.
[15] M.J. Jacquet, T. Boulier, M.A. Claude, E. Cancellieri, C. Adrados, A. Amo, S. Pigeon, Q. Glorieux, A. Bramati, E. Giacobino, Phil. Trans. R. Soc. A 378 (2020) 20190225, http://dx.doi.org/10.1098/rsta.2019.0225.
[16] M. Visser, Internat. J. Modern Phys. D 12 (4) (2003) 649–661, http://dx.doi.org/10.1142/S0218271803003190.
[17] R. Brout, S. Massar, R. Parentani, P. Spindel, Phys. Rev. D 52 (8) (1995) 4559–4568, http://dx.doi.org/10.1103/physrevd.52.4559.
[18] E. Rubino, J. McLenaghan, S.C. Kehr, F. Belgiorno, D. Townsend, S. Rohr, C. Kuklewicz, U. Leonhardt, F. König, D. Faccio, Phys. Rev. Lett. 108 (25) (2012) 253901, http://dx.doi.org/10.1103/PhysRevLett.108.253901.
[19] S. Corley, Phys. Rev. D 57 (10) (1998) 6280–6291, http://dx.doi.org/10.1103/PhysRevD.57.6280.
[20] U. Leonhardt, S. Robertson, New J. Phys. 14 (5) (2012) 053003–053015, http://dx.doi.org/10.1088/1367-2630/14/5/053003.
[21] C.W. Robson, L. Di Mauro Villari, F. Biancalana, Phys. Rev. D 99 (4) (2019) 044042, http://dx.doi.org/10.1103/PhysRevD.99.044042.
[22] C.W. Robson, L. Di Mauro Villari, F. Biancalana, The hawking temperature of anti-de Sitter black holes: Topology and phase transitions, 2019, arXiv arXiv:1903.04627.
[23] J.B. Hartle, Gravity, Pearson Education, New York, 2003, URL https://www.pearson.com/us/higher-education/program/Hartle-Gravity-An-Introduction-to-Einstein-s-General-Relativity/PGM298455.html.
[24] N. Birrell, P.C.W. Davies, Quantum Fields in Curved Space, Cambridge University Press, Cambridge, 1982, http://dx.doi.org/10.1017/CBO9780511622632.
[25] U. Leonhardt, T.G. Philbin, Lecture Notes in Phys. 718 (2007) 229–245, http://dx.doi.org/10.1007/3-540-70859-6.
[26] S. Robertson, J. Phys. B: At. Mol. Opt. Phys. 45 (16) (2012) 163001–163042, http://dx.doi.org/10.1088/0953-4075/45/16/163001.
[27] F. Biancalana, Physics 5 (2012) 68, http://dx.doi.org/10.1103/Physics.5.68.
[28] U. Leonhardt, Nature 415 (6870) (2002) 406–409, http://dx.doi.org/10.1038/415406a.
[29] G.P. Agrawal, Nonlinear Fiber Optics, fifth ed., Academic Press, New York, 2013, URL https://www.elsevier.com/books/nonlinear-fiber-optics/agrawal/978-0-12-397023-7.
[30] D. Bermudez, J. Phys. Conf. Ser. 698 (2016) 012017, http://dx.doi.org/10.1088/1742-6596/698/1/012017.
[31] W.G. Unruh, Phys. Rev. D 14 (4) (1976) 870–892, http://dx.doi.org/10.1103/PhysRevD.14.870.
[32] S. Fulling, P.C.W. Davies, Proc. R. Soc. Lond. Ser. A Math. Phys. Eng. Sci. 348 (1976) 393–414, http://dx.doi.org/10.1098/rspa.1976.0045.
[33] J. Schwinger, Phys. Rev. 82 (5) (1951) 664–679, http://dx.doi.org/10.1103/PhysRev.82.664.
[34] T. Jacobson, Phys. Rev. D 53 (12) (1996) 7082–7088, http://dx.doi.org/10.1103/PhysRevD.53.7082.
[35] T. Jacobson, Phys. Rev. D 44 (6) (1991) 1731–1739, http://dx.doi.org/10.1103/PhysRevD.44.1731.
[36] W.G. Unruh, Phys. Rev. D 51 (6) (1995) 2827–2838, http://dx.doi.org/10.1103/PhysRevD.51.2827.
[37] S. Corley, T. Jacobson, Phys. Rev. D 59 (12) (1999) 124011, http://dx.doi.org/10.1103/PhysRevD.59.124011.